Acyl-CoA oxidases fine-tune the production of ascaroside pheromones with specific side chain lengths

Xinxing Zhang†, Yuting Wang†, David H. Perez, Rachel A. Jones Lipinski, and Rebecca A. Butcher*

Department of Chemistry, University of Florida, Gainesville, FL, United States

*E-mail: <u>butcher@chem.ufl.edu</u>

†X.Z. and Y.W. contributed equally to this work.

Abstract

Caenorhabditis elegans produces a complex mixture of ascaroside pheromones to control its development and behavior. Acyl-CoA oxidases, which participate in β-oxidation cycles that shorten the side chains of the ascarosides, regulate the mixture of pheromones produced. Here, we use CRISPR-Cas9 to make specific nonsense and missense mutations in acox genes and determine the effect of these mutations on ascaroside production in vivo. Ascaroside production in acox-1.1 deletion and nonsense strains, as well as a strain with a missense mutation in a catalytic residue, confirms the central importance of ACOX-1.1 in ascaroside biosynthesis and suggests that ACOX-1.1 functions in part by facilitating the activity of other acyl-CoA oxidases. Ascaroside production in an acox-1.1 strain with a missense mutation in an ATP-binding site at the ACOX-1.1 dimer interface suggests that ATP binding is important for the enzyme to function in ascaroside biosynthesis in vivo. Ascaroside production in strains with deletion, nonsense, and missense mutations in other acox genes demonstrates that ACOX-1.1 works with ACOX-1.3 in processing ascarosides with 7-carbon side chains, ACOX-1.4 in processing ascarosides with 9carbon and 11-carbon side chains, and ACOX-3 in processing ascarosides with 13-carbon and 15-carbon side chains. It also shows that ACOX-1.2, but not ACOX-1.1, processes ascarosides with 5-carbon ω-side chains. By modeling the ACOX structures, we uncover characteristics of the enzyme active sites that govern substrate preferences. Our work demonstrates the role of specific acyl-CoA oxidases in controlling the length of ascaroside side chains and thus in determining the mixture of pheromones produced by *C. elegans*.

Key words: ascarosides; β-oxidation; acyl-CoA oxidases; CRISPR-Cas9; dauer pheromone; Caenorhabditis elegans

Introduction

The nematode *C. elegans* communicates via a complex mixture of ascaroside pheromones. These pheromones enable the worm to coordinate the development of the population by inducing the stress-resistant dauer larval stage under high population densities, as well as to control a variety of behaviors from sexual attraction to aggregation to dispersal. ¹⁻⁸ The ascarosides are derivatives of the dideoxy-L-sugar ascarylose attached to fatty acid side chains via either the terminal (ω) or penultimate (ω -1) carbon of the fatty acid. The length of these side chains, as well as the presence of various modifications on the ascarylose sugar (head groups) and on the end of the side chain (terminus groups), are critical determinants of the specific biological activities of individual ascarosides. ⁹ Peroxisomal β -oxidation cycles shorten the side chains of long-chain ascarosides by two carbons per cycle to produce the short-chain ascaroside pheromones. ¹⁰⁻¹⁵ The first step in these β -oxidation cycles is catalyzed by specific acyl-CoA oxidases, which install an α - β double bond in their substrates and have different side-chain length preferences. ¹²⁻¹⁵ These acyl-CoA oxidases play a critical role in determining the mixture of pheromones produced by the worm.

The *C. elegans* genome encodes seven acyl-CoA oxidases, with four of them clustered on chromosome I (**Fig. 1**). Because of their homology to mammalian ACOX-1, the acyl-CoA oxidases that were previously referred to as ACOX-1,-2,-3,-4, and -5¹²⁻¹⁵ have been renamed ACOX-1.1,-1.2, -1.3, -1.4, and -1.5, respectively, and another acyl-CoA oxidase (F59F4.1) has been named ACOX-1.6 (Table S1). Because of its homology to mammalian ACOX-3, the acyl-CoA oxidase that was previously referred to as ACOX-6¹⁵ has been renamed ACOX-3 (Table S1). The latter three steps in each β -oxidation cycle are catalyzed by an enoyl-CoA hydratase (MAOC-1), a (3*R*)-hydroxyacyl-CoA dehydrogenase (DHS-28), and a 3-ketoacyl-CoA thiolase

(DAF-22).¹⁰⁻¹⁴ Previous work from our group has shown that (ω-1)-ascarosides and ω-ascarosides are biosynthesized by two parallel β-oxidation pathways (**Fig. 2A,B**).¹⁴ The acyl-CoA oxidases involved in these pathways are thought to form homo and heterodimer complexes. Genetic evidence has implicated ACOX-1.1 in the processing of ascarosides with long- and medium-length (ω-1)- and ω-side chains.¹²⁻¹⁴ Biochemical evidence has confirmed that an ACOX-1.1 homodimer processes an ascaroside with a 9-carbon (ω-1)-side chain (asc-C9-CoA) and that an ACOX-1.1/ACOX-1.3 heterodimer processes an ascaroside with a 7-carbon (ω-1)-side chain (asc-C7-CoA) *in vitro* (**Fig. 2A**).¹⁴ Genetic evidence has also implicated ACOX-1.1 and ACOX-1.2 in the processing of an ascaroside with a 5-carbon ω-side chain, asc-ωC5-CoA.¹³. However, while an ACOX-1.2 homodimer was specifically active towards asc-ωC5-CoA *in vitro* (**Fig. 2B**), an ACOX-1.1 homodimer showed no activity towards this substrate.¹⁴

The crystal structures of an ACOX-1.1 homodimer bound to its FAD cofactor, as well as an ACOX-1.2 homodimer bound to its FAD cofactor and preferred substrate (asc-ωC5-CoA), have been reported. ¹⁵ Consistent with its ability to process substrates with a range of side chain lengths, the ACOX-1.1 homodimer structure has a large active site that opens to two channels on the outer surface of the protein. ¹⁵ On the other hand, the ACOX-1.2 homodimer has a smaller active site that is mostly closed off from the outer surface of the protein and that has specific active site residues that recognize the ascarylose sugar of its preferred short-chain substrate. ¹⁵ Interestingly, both the ACOX-1.1 and ACOX-1.2 homodimer structures revealed two ATP molecules bound at the dimer interface. The ATP binding residues are conserved in most *C. elegans* acyl-CoA oxidases. Mutation of the ATP binding site of ACOX-1.1 reduces the binding of the enzyme to ATP and the FAD cofactor and reduces its *in vitro* enzymatic activity. ¹⁵

Transcriptional regulation of the acyl-CoA oxidases appears to be important for the regulation of ascaroside production. The expression of acox-1.1 is downregulated in males, thereby allowing the accumulation of the male-produced sex pheromone asc-C9 (ascr#10).¹⁶ Although the production of most ascarosides is increased with the addition of food, the expression of acox-1.3 is downregulated by food, thereby suppressing increased production of the short-chain, (ω -1)-ascarosides, including the dauer pheromone asc-C6-MK (ascr#2).¹⁴ Interestingly, the expression of acox-1.2 and the production of asc- ω C3 (ascr#5) is induced by favorable, non-dauer-inducing conditions (low population density/ high food), despite the dauer-inducing activity of asc- ω C3.¹⁴ Unlike other dauer pheromones, asc- ω C3 has a side chain that is attached at its ω -position (rather than (ω -1)-position) to the ascarylose, and intriguingly, this ascaroside works synergistically with the others to induce dauer formation, and targets a unique class of GPCRs.^{3, 17-19}

Our data show that the ACOX-1.1 protein itself is more critical for ascaroside biosynthesis than the catalytic activity of the enzyme, indicating that the ACOX-1.1 protein may function in part by promoting the catalytic activity of *other* acyl-CoA oxidases, possibly by forming a heterodimer complex with them. Our data show that ACOX-1.1, works with ACOX-1.3, ACOX-1.4, and ACOX-3 in the β -oxidation pathway for $(\omega$ -1)-ascarosides and with ACOX-1.2 in the β -oxidation pathway for ω -ascarosides. We implicate ACOX-1.4 and ACOX-3 for the first time in ascaroside biosynthesis, providing evidence that ACOX-1.4 works with ACOX-1.1 in the processing of ascarosides with 9- and 11-carbon (ω -1)-side chains and that ACOX-3 works with ACOX-1.1 in the processing of ascarosides with 13- and 15-carbon (ω -1)-side chains. Furthermore, we show that ACOX-1.1 does not play a role in processing 5-carbon ω -ascarosides, whereas ACOX-1.2 does. Thus, ACOX-1.2 is the key player in the production of

the short-chain ω -ascaroside and potent dauer pheromone, asc- ω C3. Lastly, we develop homology models of the protein structures of ACOX-1.3, ACOX-1.4, and ACOX-3, and show that these structures are consistent with the proposed activities of the enzymes.

Results and Discussion

Role of acox-1.1 and acox-1.2 in processing short-chain ascarosides. Previously, we and others have analyzed ascaroside production of the acox-1.1(ok2257) deletion mutant, and these data suggested that acox-1.1 plays a role in the processing of longer chain ascarosides, as well as in processing $(\omega-1)$ -ascarosides with 9-carbon side chains, $(\omega-1)$ -ascarosides with 7-carbon side chains, and ω-ascarosides with 5-carbon side chains. ^{13, 14} However, the clustering of the acox-1.1, -1.2, -1.3, and -1.4 genes on chromosome I complicates the interpretation of these data. The deletion in the acox-1.1(ok2257) deletion mutant could potentially interfere with the expression of the nearby acox-1.2 gene, which is important for the conversion of anω-ascaroside with a 5carbon side chain to one with a 3-carbon side chain.¹⁴ To investigate further the role of ACOX-1.1 in the biosynthesis of short-chain ω-ascarosides, we generated several acox-1.1 mutant strains using the genome-editing technique, CRISPR-Cas9 (Fig. 1).²⁰⁻²² First, we generated a nonsense mutant, acox-1.1(stop), which is unlikely to affect the expression of acox-1.2 through disruption of the acox-1.2 promoter, given that it is a small mutation near the 5'-end of the acox-1.1 gene (Fig. 3A and Fig. S1). Analysis of ascaroside production in this strain indicates that acox-1.1 does not play a role in processing a 5-carbon ω-ascaroside to a 3-carbon ω-ascaroside (Fig. 3A). This result is consistent with our biochemical data that showed that an ACOX-1.2 homodimer is specifically active towards asc-ωC5-CoA, while an ACOX-1.1 homodimer is

inactive towards this substrate (**Fig. 2A,B**). ¹⁴ Thus, ACOX-1.2, not ACOX-1.1, is the key acyl-CoA oxidase controlling the production of the dauer pheromone asc- ω C3 (ascr#5).

Surprisingly, a missense mutant strain, acox-1.1(E434A), in which the catalytic Glu-434 is mutated to an Ala, produced ascarosides at similar levels to wild type, except for a slight accumulation of medium chain-length (C11) ascarosides (**Fig. 3A** and **Fig. S2**). Unlike the acox-1.1(stop) nonsense strain, the missense strain did not accumulate asc-C7 and asc-C9. When the ACOX-1.1(E434A) mutant enzyme was expressed in $E.\ coli$ and purified, it had almost no activity (**Fig. S3**). The very mild phenotype of the acox-1.1(E434A) catalytic mutant suggests that the ACOX-1.1 catalytic activity is less important than the actual ACOX-1.1 protein for the biosynthesis of the ascarosides, and that the catalytic activity of other acyl-CoA oxidases can compensate for the absence of catalytically active ACOX-1.1. The key role of ACOX-1.1 may be to promote the folding and/or enzymatic activity of other acyl-CoA oxidases.

Role of ATP-binding by ACOX-1.1 in ascaroside biosynthesis. To further examine the role of ACOX-1.1, we made another missense mutant, acox-1.1(H396G), in which His-396 is mutated to a Gly (Fig. 3B and Fig. S4). As shown in the crystal structure of ACOX-1.1, this His is important for the binding of an ATP molecule at the interface between the two subunits in the ACOX-1 homodimer. The ATP binding pocket is highly conserved in other acyl-CoA oxidases in *C. elegans*, except for ACOX-3 (previously referred to as ACOX-6). Although the ACOX-1.1(H396G) mutant enzyme can be expressed in *E. coli* and purified as a well-folded homodimer, it does not bind the FAD cofactor as well. Furthermore, the mutant enzyme shows significantly reduced activity towards both fatty acyl-CoA and ascaroside-CoA substrates. The acox-1.1(H396G) missense mutant has a similar phenotype in terms of ascaroside production as

does the *acox-1.1(stop)* nonsense mutant, displaying defects in the processing of (ω-1)-ascarosides with 13-carbon, 11-carbon, 9-carbon, and 7-carbon side chains (**Fig. 3B**). This result suggests that ATP binding is necessary for ACOX-1.1 to participate in ascaroside biosynthesis and/or to promote the activity of other acyl-CoA oxidases. We verified that the ascaroside production defects of the *acox-1.1(H396G)* mutant strain are not likely due to an inability of this strain to express ACOX-1.1. We generated two translational reporter strains, *acox-1.1p::gfp::acox-1.1* and *acox-1.1p::gfp::acox-1.1(H396G)*, and showed that both strains displayed a similar punctate pattern of GFP expression in the peroxisome (**Fig. S5**). Given that ACOX-1.1 has a C-terminal peroxisomal targeting sequence, it is likely that ACOX-1.1 is expressed properly in both reporter strains. Our previous results showed that ATP binding is important *in vitro* for ACOX-1.1 to contribute to ascaroside biosynthesis, ¹⁵ and our results here suggest that ATP binding is important *in vitro* as well.

Role of *acox-1.3* and *acox-1.4* in processing -medium-chain ascarosides. Previously, we showed that an *acox-1.3(tm5192)* deletion mutant accumulates asc-C7 and makes less asc- Δ C7, indicating that ACOX-1.3 participates in the β -oxidation cycle that converts an (ω -1)-ascaroside with a 7-carbon side chain to one with a 5-carbon side chain (**Fig. 2A**). Furthermore, an ACOX-1.1/ACOX-1.3 heterodimer is specifically active towards asc-C7-CoA. Ascaroside production in the *acox-1.3(stop)* nonsense mutant is very consistent with that in the *acox-1.3(tm5192)* deletion mutant, further supporting the proposed role of ACOX-1.3 in ascaroside biosynthesis (**Fig. 4A** and **Fig. S6**).

The *acox-1.4(tm6415)* deletion strain, the *acox-1.4(stop)* nonsense mutant, and the *acox-1.4(E433A)* catalytic mutant all accumulate asc-C9, indicating that ACOX-1.4 participates in the

 β -oxidation cycle that converts an (ω-1)-ascaroside with a 9-carbon side chain to one with a 7carbon side chain (Fig. 4B and Fig. S7). Although the acox-1.4(tm6415) deletion mutant also accumulates asc-C7, this increase may be due to the effect of this deletion on the expression of acox-1.3. In support of this hypothesis, an acox-1.3(rab5); acox-1.4(tm6415) double deletion mutant displayed similar ascaroside production as either of the two single deletion mutants (data not shown). To further investigate the role of acox-1.4, we compared ascaroside production in the acox-1.1(E434A) catalytic mutant and acox-1.4(E433A) catalytic mutant to that in the acox-1.1(E434A); acox-1.4(E433A) double mutant (Fig. S8). These data show that the catalytic activity of both acox-1.1 and acox-1.4 contributes to the processing of asc-C9, as well as asc-C11. However, it shows that the catalytic activity of acox-1.4 is more important for the processing of asc-C9, while the catalytic activity of acox-1.1 is more important for the processing of asc-C11. These data also provide further confirmation that acox-1.4 does not contribute to the processing of asc-C7. Unfortunately, our repeated attempts to express ACOX-1.4, either alone or co-expressed with other acyl-CoA oxidases, in E. coli have been unsuccessful, and thus we have been unable to test its enzymatic activity in vitro.

Role of *acox-1.1* and *acox-3* in processing long-chain ascarosides. In order to implicate additional acyl-CoA oxidases in the biosynthesis of the ascarosides, we analyzed ascaroside production in mutants of *acox-1.5*, *acox-1.6*, and *acox-3*. The *acox-1.5*(*ok2619*) and *acox-1.6*(*ok2119*) deletion mutants did not show any defects in ascaroside production (**Fig. S9**). On the other hand, the *acox-3*(*tm4033*) deletion mutant did show some mild defects in the production of medium-chain ascarosides (**Fig. 5**, **Fig. S10**). Therefore, we decided to make a double mutant of *acox-1.1* and *acox-3*. *acox-3* is the least similar to other acyl-CoA oxidases in

C. elegans, and previous RNAi experiments analyzing for specific ascarosides suggested that this gene is not involved in ascaroside biosynthesis. However, comparison of ascaroside production in the acox-1.1(ok2257); acox-3(tm4033) double deletion mutant to the acox-1.1(ok2257) single deletion mutant demonstrates that acox-3 contributes to the shortening of (ω-1)-ascarosides with 13- and 15-carbon side chains (Fig. 5). Comparison of the acox-1.1(E434A); acox-3(tm4033) double mutant to the acox-1.1(E434A) single mutant further suggests a role for acox-3 in the processing of (ω-1)-ascarosides with 13- and 15-carbon side chains (Fig. S10). Comparison of the acox-1.1(E434A); acox-3(tm4033) double mutant to the acox-3(tm4033) single mutant also shows that ACOX-1.1's catalytic function plays a role in the shortening of (ω-1)-ascarosides with 13- and 15-carbon side chains (Fig. S10). Thus, our genetic data suggest that ACOX-1.1 catalytic function is more important for longer chain ascarosides (C11-C15) than it is for shorter chain ascarosides (C7-C9). This conclusion is further supported by the fact that ACOX-1.1 is more active towards asc-C13-CoA than it is towards asc-C9-CoA in vitro (Fig. S3).

Modeling of the acyl-CoA oxidase active sites. Previously, we published the crystal structures of the ACOX-1.1 homodimer bound to FAD and ATP and the crystal structure of the ACOX-1.2 homodimer bound to FAD, ATP, and a short-chain ascaroside substrate (asc-ωC5-CoA). As we previously established, the ACOX-1.1 active site opens to two channels that run along the outer surface of the protein, and we speculated that these channels enable the enzyme to accommodate longer fatty acid and ascaroside substrates (Fig. 6A-C). Conversely, the ACOX-1.2 active site is much smaller and is closed to the outer surface of the protein (Fig. 6B). This small active site limits the substrate range of ACOX-1.2 to the short-chain ω-ascaroside, asc-

ωC5-CoA. In order to evaluate whether the active sites of the acyl-CoA oxidases are consistent with the substrate preferences suggested by the ascaroside profiles of the *acox* mutants, we developed a homology model of the structures of ACOX-1.3 and ACOX-1.4, primarily using the ACOX-1.2 crystal structure (**Fig. 6C,D**). We also developed a homology model of the ACOX-3 structure, primarily using the crystal structure of an acyl-CoA oxidase from *Lycopersicon esculentum* (tomato), LeACX1 (**Fig. 6E**). ACOX-1.3 and ACOX-1.4 both have 81% sequence identity to ACOX-1.2, while ACOX-3 has 31% sequence identity to LeACX1. Although the latter is relatively low, the modeling program that we used, RaptorX is was specifically developed for the modeling of proteins with less than 30% sequence identity.²³⁻²⁵

The predicted ACOX-1.3 structure suggests that the active site is relatively small, is largely enclosed, and is consistent with the small size of its preferred substrate, asc-C7-CoA (Fig. 6C). The predicted ACOX-1.4 structure has an active site that is similar in size to that of ACOX-1.1, and both active sites are open to the outer surface of the protein (Fig. 6D). Thus, it is not surprising that ACOX-1.1 and ACOX-1.4 are implicated in the processing of the substrates asc-C9-CoA and asc-C11-CoA. ACOX-3 is only distantly related to the remaining acyl-CoA oxidases, and its modeled active site displays a larger opening to the outer surface of the protein and larger channels on the outer surface (Fig. 6E). This large, open active site may enable ACOX-3 to contribute to the processing of long-chain (C13, C15) ascarosides, as well as possibly, additional larger substrates.

Conclusions

In order to control the ascaroside mixture produced under different conditions, C. elegans must carefully regulate the β -oxidation cycles that determine the length of the ascaroside side

chains. Earlier work showed that ACOX-1.1 plays an important role in processing ω - and (ω -1)-ascarosides with a broad range of side chain lengths. ¹²⁻¹⁵ Given that acox-1.1 deletion and nonsense mutant strains show much stronger defects in ascaroside production than an acox-1.1 catalytic mutant strain, our data suggest that ACOX-1.1 plays additional roles in ascaroside biosynthesis beyond its catalytic function. For example, ACOX-1.1 may facilitate the expression or folding of other acyl-CoA oxidases, or may serve as a scaffold, forming heterodimers with other acyl-CoA oxidases and facilitating their activity, as our earlier data have suggested. ¹⁴ The acox-1.1 missense mutant strain which expressed ACOX-1.1 with a mutation (H396G) in its ATP-binding site showed strong defects in ascaroside biosynthesis, providing evidence that ATP binding is important for ACOX-1.1 to contribute to ascarosides biosynthesis not only *in vitro* (as had been shown previously), ¹⁵ but also *in vivo*.

In terms of the biosynthesis of ω -ascarosides, our data show that ACOX-1.2 is dedicated to the processing of ascarosides with 5-carbon ω -side chains while ACOX-1.1 functions in the processing of those with \geq 7-carbon ω -side chains. Specifically, we showed that unlike the *acox-1.1* deletion mutant strain, *acox-1.1* nonsense and missense mutant strains did not show defects in processing asc- ω C5. Thus, our genetic data are in agreement with our previous biochemical data which showed that ACOX-1.2 could process an asc- ω C5-CoA substrate while ACOX-1.1 could process longer chain ω -ascarosides, such as asc- ω C7-CoA. 14, 15 In terms of the biosynthesis of (ω -1)-ascarosides, our data show that ACOX-1.1, ACOX-1.3, ACOX-1.4, and ACOX-3 play important roles. Ascaroside production in *acox-1.1* and *acox-1.3* nonsense mutant strains confirmed previous data that ACOX-1.3 functions with ACOX-1.1 in the processing of ascarosides with 7-carbon (ω -1)-side chains. Ascaroside production in *acox-1.4* nonsense and catalytic mutant strains, as well as in an *acox-1.1;acox-1.4* double mutant strain, demonstrated

that ACOX-1.4 works with ACOX-1.1 in the processing of ascarosides with 9- and 11-carbon (ω-1)-side chains. Ascaroside production in the *acox-1.1;acox-3* double mutant, in comparison to the *acox-1.1* single mutant, suggested that ACOX-3 works with ACOX-1.1 in the processing of ascarosides with 13- and 15-carbon (ω-1)-side chains. The modeled ACOX-1.3 active site is small and closed to the outer surface of the protein while the modeled ACOX-1.4 and ACOX-3 active sites are larger and open to the outer surface, perhaps explaining why the latter enzymes are able to accommodate ascaroside substrates with longer side chains. In summary, our current work clarifies the substrate preferences of ACOX-1.1, ACOX-1.2, and ACOX-1.3 and also implicates additional acyl-CoA oxidases, ACOX-1.4 and ACOX-3, in ascaroside biosynthesis. Overall, we demonstrate that acyl-CoA oxidases provide a much finer level of control of sidechain length than previously appreciated.

Material and Methods

C. elegans strains. The following strains were used: wild-type (N2, Bristol), VC1785 acox-1.1 (ok2257) I, acox-1.1(rab1, stop) I, acox-1.1(rab2, E434A) I, acox-1.1(rab3, H396G) I, VC20731 acox-1.2(gk386052) I, acox-1.3(tm5192) I, acox-1.3(rab4, stop) I, acox-1.4(tm6415) I, VC40944 acox-1.4(gk892586) I, acox-1.4(rab6, E433A) I, acox-1.5(ok2619) III, acox-3(tm4033) IV, acox-1.6(ok2119) X, acox-1.3(rab4, stop); acox-1.4(tm6415), acox-1.1(ok2257); acox-3(tm4033), acox-1.1(rab2; E434A); acox-1.4(rab6, E433A), acox-1.1(rab2; E434A); acox-3(tm4033). The acox-1.1(ok2257), acox-1.3(tm5192), acox-1.4(tm6415), acox-1.5(ok2619), and acox-3(tm4033) strains were backcrossed four or six times. The nonsense mutations in the acox-1.2(gk386052) and acox-1.4(gk892586) strains, which were generated in the Million Mutation Project, ²⁶ were verified by sequencing a genomic PCR fragment. The acox-1.1(rab1, stop), acox-1.1(rab2;

E434A), acox-1.3(rab3, H396G), and acox-1.4(rab6, E433A) mutants were generated using CRISPR-Cas9 and backcrossed two to six times. The acox-1.3(rab5); acox-1.4(tm6415) strain was made using CRISPR-Cas9 by generating the acox-1.3(rab5) deletion in the acox-1.4(tm6415) background. The acox-1.1(rab2, E434A); acox-1.4(rab6, E433A) strain was made using CRISPR-Cas9 by generating the acox-1.1(rab2, E434A) mutation in the acox-1.4(rab6, E433A) background.

CRISPR-Cas9. All CRISPR-Cas9 mutants were made using the Fire laboratory's marker-free CRISPR protocol. ^{20-22, 27} The Cas9 vector was injected at 50 ng μL⁻¹, all sgRNA vectors were at 25 ng μL⁻¹, the *dpy-10 cn64* donor oligonucleotide was at 500 nM, and custom donor plasmids were at 50 ng μL⁻¹. Custom sgRNAs were designed using Feng Zhang's CRISPR design tool (http://crispr.mit.edu/). ²⁷ Custom donor plasmids, which were constructed in the pPD95.75 vector (from Andy Fire, via Addgene), included homologous arms with about 500 bases and introduced a restriction site along with the desired mutation. The F1 Rol and Dpy worms were checked by PCR and digestion. The PCR products of candidate worms were then sequenced for the desired mutations (**Fig. S1, S2, S4, S6, and S7**). Finally, the Dpy phenotype was crossed out with wild-type worms.

Ascaroside analysis of large-scale cultures. Large-scale (150 mL) non-synchronized worm cultures were fed $E.\ coli$ (HB101) and grown for 9 d, and extracts were generated from the culture medium, as described. LC-MS/MS analysis of ascarosides from extracts was performed as described, but with some modifications. A Phenomenex Kinetex 2.6 μ M C18 100Å (100 × 2.1 mm) column was attached to an Accela UHPLC and a Thermo TSQ Quantum

Max mass spectrometer, operating in negative ion, heated (H)-ESI, precursor scanning mode (selecting for a product ion of m/z 73.0). Quantitation of ascarosides by LC-MS/MS was done by generating a calibration curve using synthetic standards. All ascarosides were quantified using their corresponding synthetic standard, except for asc-C13 and asc-C15, which were quantitated using synthetic asc-C11.

Ascaroside analysis of small-scale cultures. For Figure S8-S10, small-scale (5 mL) non-synchronized worm cultures were started with worms from one 6 cm NGM-agar plate, fed *E. coli* (HB101), and grown for 7 d. For sample collection, 5 mL of culture was centrifuged (800g for 2 min), the worms at the bottom were removed, and the supernatant was centrifuged again (3500 rpm for 10 min). 1 mL of this supernatant was lyophilized and resuspended in 100 μL of 50% methanol in water, and the ascarosides were analyzed by LC-MS as described.²⁸ LC-MS analysis of ascarosides was performed on a Phenomenex Luna 5 μm C18 (2) 100 Å (100 x 4.6 mm) column attached to an Agilent 1260 infinity binary pump and Agilent 6130 single quad mass spectrometer with API-ES source, operating in dual negative/positive, ESI, single-ion monitoring mode, as previously described.¹⁴ In general, all ascarosides were detected by LC-MS using the [M-H]⁻ ion.

acox-1.1 and acox-1.1(H396G) translational reporter strains. 2 kb of the acox-1.1 promoter and 4 kb of the acox-1.1 gene plus 3'-UTR were inserted into the Sall/NotI and NgoMIV/ApaI sites, respectively, of pPD114.108 (from A. Fire, via Addgene). The point mutation was made using the Q5 site-directed mutagenesis kit (New England Biolabs), following the manufacturer's instructions. 50 ng μL⁻¹ of the transgenes and 50 ng μL⁻¹ of the co-injection marker unc-

122p::DsRed (gift of P. Sengupta) were injected into wild-type worms. At least three independent transgenic strains were analyzed. Imaging was conducted on a Zeiss Axiovert.A1 microscope equipped with an AxioCam ICm1 camera.

Acolayle CoA oxidase expression and activity assay. The cloning and expression conditions for ACOX-1.1a (the longest splice variant of ACOX-1.1) and the ACOX-1.1a (E434A) catalytic mutant were described previously. Ascarosides were synthesized as described previously. CoA-thioesters of ascarosides were synthesized as described previously, except for asc-C13-CoA which was synthesized chemoenzymatically using the fatty acyl-CoA ligase FadD6. Briefly, the FadD6 gene was amplified by PCR from a *Mycobacterium tuberculosis* H37Ra genomic library (a gift from P. Zhang and Y. Ding), cloned into the pET28a vector using the Ndel/NotI sites, and expressed and purified using a similar method as was used for the acyl-CoA oxidases, we except that expression was induced overnight at 20°C and FAD was not included in protein purification buffers. For a 200 μL total reaction volume, ~300 μM asc-C13, 5 mM CoA, 15 mM ATP and 20 μg FadD6 protein were added to reaction buffer (100 mM Tris, 8 mM MgCl₂, pH 7.5), and the reaction was incubated at 30°C for 1h. The product was purified by HPLC. The acyl-CoA oxidase activity assay was performed as described previously, were performed at room temperature (~23°C).

Acyl-CoA oxidase structure prediction. The amino acid sequence of each acyl-CoA oxidase was provided to the RaptorX Structure Prediction server, ^{23-25, 30} and the resulting structure was visualized using Visual Molecular Dynamics (VMD) software. ³¹ Using the STAMP method ³² in the MultiSeq feature of VMD, the predicted structures were aligned to the ACOX-1.1 and

ACOX-1.2 crystal structures, and this alignment was done independently for each monomer of the homodimeric structure. The individually aligned structures were then combined to form predicted structures for the ACOX-1.3, ACOX-1.4, and ACOX-3 dimers.

Author contributions. R.A.B., X.Z., and Y.W. designed the experiments and analyzed data; X.Z. and Y.W. performed experiments; D.H.P. performed protein modeling; R.A.J. provided reagents; R.A.B. and X.Z. wrote the paper, which was reviewed by all authors.

Acknowledgments. We thank P. McGrath and W. Xu for kindly providing plasmids and advice for making mutations via CRISPR-Cas. We also thank A. Fire and P. Sengupta for plasmids. We are grateful to T. Garrett and the Southeast Center for Integrated Metabolomics for access to the LC-MS/MS. Some strains were provided by S. Mitani at the National Bioresource Project (Japan) and by the Caenorhabditis Genetics Center, which is funded by the NIH Office of Research Infrastructure Programs (P40 OD010440). This work was supported by the NSF (Career 1555050), the Ellison Medical Foundation, the Research Corporation for Science Advancement, and the Alfred P. Sloan Foundation.

Supporting Information Available: This material is available free of charge via the Internet.

Supporting Figures S1-S10 and Table S1

References

[1] Jeong, P. Y., Jung, M., Yim, Y. H., Kim, H., Park, M., Hong, E., Lee, W., Kim, Y. H., Kim, K., and Paik, Y. K. (2005) Chemical structure and biological activity of the *Caenorhabditis elegans* dauer-inducing pheromone, *Nature 433*, 541-545.

- [2] Butcher, R. A., Fujita, M., Schroeder, F. C., and Clardy, J. (2007) Small-molecule pheromones that control dauer development in *Caenorhabditis elegans*, *Nat Chem Biol 3*, 420-422.
- [3] Butcher, R. A., Ragains, J. R., Kim, E., and Clardy, J. (2008) A potent dauer pheromone component in *C. elegans* that acts synergistically with other components, *Proc Natl Acad Sci U S A 105*, 14288-14292.
- [4] Butcher, R. A., Ragains, J. R., and Clardy, J. (2009) An indole-containing dauer pheromone component with unusual dauer inhibitory activity at higher concentrations, *Org Lett 11*, 3100-3103.
- [5] Pungaliya, C., Srinivasan, J., Fox, B. W., Malik, R. U., Ludewig, A. H., Sternberg, P. W., and Schroeder, F. C. (2009) A shortcut to identifying small molecule signals that regulate behavior and development in *Caenorhabditis elegans*, *Proc Natl Acad Sci U S A 106*, 7708-7713.
- [6] Srinivasan, J., Kaplan, F., Ajredini, R., Zachariah, C., Alborn, H. T., Teal, P. E., Malik, R. U., Edison, A. S., Sternberg, P. W., and Schroeder, F. C. (2008) A blend of small molecules regulates both mating and development in *Caenorhabditis elegans*, *Nature* 454, 1115-1118.
- [7] Srinivasan, J., von Reuss, S. H., Bose, N., Zaslaver, A., Mahanti, P., Ho, M. C., O'Doherty, O. G., Edison, A. S., Sternberg, P. W., and Schroeder, F. C. (2012) A modular library of small molecule signals regulates social behaviors in *Caenorhabditis elegans*, *PLoS Biol* 10, e1001237.
- [8] Artyukhin, A. B., Yim, J. J., Srinivasan, J., Izrayelit, Y., Bose, N., von Reuss, S. H., Jo, Y., Jordan, J. M., Baugh, L. R., Cheong, M., Sternberg, P. W., Avery, L., and Schroeder, F. C. (2013) Succinylated octopamine ascarosides and a new pathway of biogenic amine metabolism in *Caenorhabditis elegans*, *J Biol Chem 288*, 18778-18783.
- [9] Hollister, K. A., Conner, E. S., Zhang, X., Spell, M., Bernard, G. M., Patel, P., de Carvalho, A. C., Butcher, R. A., and Ragains, J. R. (2013) Ascaroside activity in *Caenorhabditis elegans* is highly dependent on chemical structure, *Bioorg Med Chem 21*, 5754-5769.
- [10] Butcher, R. A., Ragains, J. R., Li, W., Ruvkun, G., Clardy, J., and Mak, H. Y. (2009) Biosynthesis of the *Caenorhabditis elegans* dauer pheromone, *Proc Natl Acad Sci U S A* 106, 1875-1879.
- [11] Joo, H. J., Yim, Y. H., Jeong, P. Y., Jin, Y. X., Lee, J. E., Kim, H., Jeong, S. K., Chitwood, D. J., and Paik, Y. K. (2009) *Caenorhabditis elegans* utilizes dauer pheromone biosynthesis to dispose of toxic peroxisomal fatty acids for cellular homoeostasis, *Biochem J* 422, 61-71.

- [12] Joo, H. J., Kim, K. Y., Yim, Y. H., Jin, Y. X., Kim, H., Kim, M. Y., and Paik, Y. K. (2010) Contribution of the peroxisomal *acox* gene to the dynamic balance of daumone production in *Caenorhabditis elegans*, *J Biol Chem* 285, 29319-29325.
- [13] von Reuss, S. H., Bose, N., Srinivasan, J., Yim, J. J., Judkins, J. C., Sternberg, P. W., and Schroeder, F. C. (2012) Comparative metabolomics reveals biogenesis of ascarosides, a modular library of small-molecule signals in *C. elegans*, *J Am Chem Soc* 134, 1817-1824.
- [14] Zhang, X., Feng, L., Chinta, S., Singh, P., Wang, Y., Nunnery, J. K., and Butcher, R. A. (2015) Acyl-CoA oxidase complexes control the chemical message produced by *Caenorhabditis elegans*, *Proc Natl Acad Sci U S A 112*, 3955-3960.
- [15] Zhang, X., Li, K., Jones, R.A., Bruner, S.D., Butcher, R.A. (2016) Structural characterization of acyl-CoA oxidases reveals a direct link between pheromone biosynthesis and metabolic state in *C. elegans*, *Proc. Natl. Acad. Sci., U.S.A. 113*, 10055-10060.
- [16] Izrayelit, Y., Srinivasan, J., Campbell, S. L., Jo, Y., von Reuss, S. H., Genoff, M. C., Sternberg, P. W., and Schroeder, F. C. (2012) Targeted metabolomics reveals a male pheromone and sex-specific ascaroside biosynthesis in *Caenorhabditis elegans*, *ACS Chem Biol* 7, 1321-1325.
- [17] Kim, K., Sato, K., Shibuya, M., Zeiger, D. M., Butcher, R. A., Ragains, J. R., Clardy, J., Touhara, K., and Sengupta, P. (2009) Two chemoreceptors mediate developmental effects of dauer pheromone in *C. elegans*, *Science* 326, 994-998.
- [18] McGrath, P. T., Xu, Y., Ailion, M., Garrison, J.L., Butcher, R.A., Bargmann, C.I. (2011) Parallel evolution of domesticated *Caenorhabditis* species targets pheromone receptor genes, *Nature* 477, 321-325.
- [19] Park, D., O'Doherty, I., Somvanshi, R. K., Bethke, A., Schroeder, F. C., Kumar, U., and Riddle, D. L. (2012) Interaction of structure-specific and promiscuous G-protein-coupled receptors mediates small-molecule signaling in *Caenorhabditis elegans*, *Proc Natl Acad Sci U S A 109*, 9917-9922.
- [20] Arribere, J. A., Bell, R. T., Fu, B. X., Artiles, K. L., Hartman, P. S., and Fire, A. Z. (2014) Efficient marker-free recovery of custom genetic modifications with CRISPR/Cas9 in *Caenorhabditis elegans, Genetics* 198, 837-846.
- [21] Farboud, B., and Meyer, B. J. (2015) Dramatic enhancement of genome editing by CRISPR/Cas9 through improved guide RNA design, *Genetics* 199, 959-971.

- [22] Kim, H., Ishidate, T., Ghanta, K. S., Seth, M., Conte, D., Jr., Shirayama, M., and Mello, C. C. (2014) A co-CRISPR strategy for efficient genome editing in *Caenorhabditis elegans*, *Genetics* 197, 1069-1080.
- [23] Peng, J., and Xu, J. (2011) RaptorX: exploiting structure information for protein alignment by statistical inference, *Proteins 79 Suppl 10*, 161-171.
- [24] Kallberg, M., Wang, H., Wang, S., Peng, J., Wang, Z., Lu, H., and Xu, J. (2012) Template-based protein structure modeling using the RaptorX web server, *Nat Protoc* 7, 1511-1522.
- [25] Ma, J., Wang, S., Zhao, F., and Xu, J. (2013) Protein threading using context-specific alignment potential, *Bioinformatics* 29, i257-265.
- [26] Thompson, O., Edgley, M., Strasbourger, P., Flibotte, S., Ewing, B., Adair, R., Au, V., Chaudhry, I., Fernando, L., Hutter, H., Kieffer, A., Lau, J., Lee, N., Miller, A., Raymant, G., Shen, B., Shendure, J., Taylor, J., Turner, E. H., Hillier, L. W., Moerman, D. G., and Waterston, R. H. (2013) The million mutation project: a new approach to genetics in *Caenorhabditis elegans, Genome Res* 23, 1749-1762.
- [27] Cong, L., and Zhang, F. (2015) Genome engineering using CRISPR-Cas9 system, *Methods Mol Biol 1239*, 197-217.
- [28] Zhang, X., Noguez, J. H., Zhou, Y., and Butcher, R. A. (2013) Analysis of ascarosides from *Caenorhabditis elegans* using mass spectrometry and NMR spectroscopy, *Methods Mol Biol 1068*, 71-92.
- [29] Arora, P., Vats, A., Saxena, P., Mohanty, D., and Gokhale, R. S. (2005) Promiscuous fatty acyl CoA ligases produce acyl-CoA and acyl-SNAC precursors for polyketide biosynthesis, *J Am Chem Soc* 127, 9388-9389.
- [30] Peng, J., and Xu, J. (2011) A multiple-template approach to protein threading, *Proteins* 79, 1930-1939.
- [31] Humphrey, W., Dalke, A., and Schulten, K. (1996) VMD: visual molecular dynamics, *J Mol Graph 14*, 33-38, 27-38.
- [32] Roberts, E., Eargle, J., Wright, D., and Luthey-Schulten, Z. (2006) MultiSeq: unifying sequence and structure data for evolutionary analysis, *BMC Bioinformatics* 7, 382.

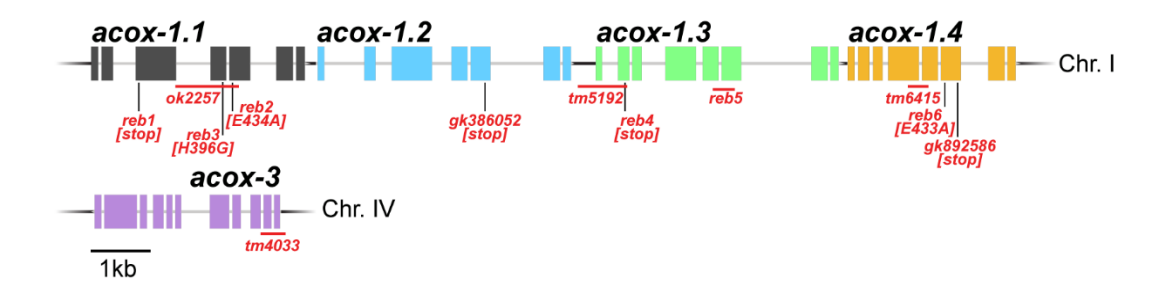


Figure 1. Gene structure of acyl-CoA oxidases in *C. elegans* with description of acox mutants used in this study and one analyzed previously (acox-1.2(gk386052)).¹⁴

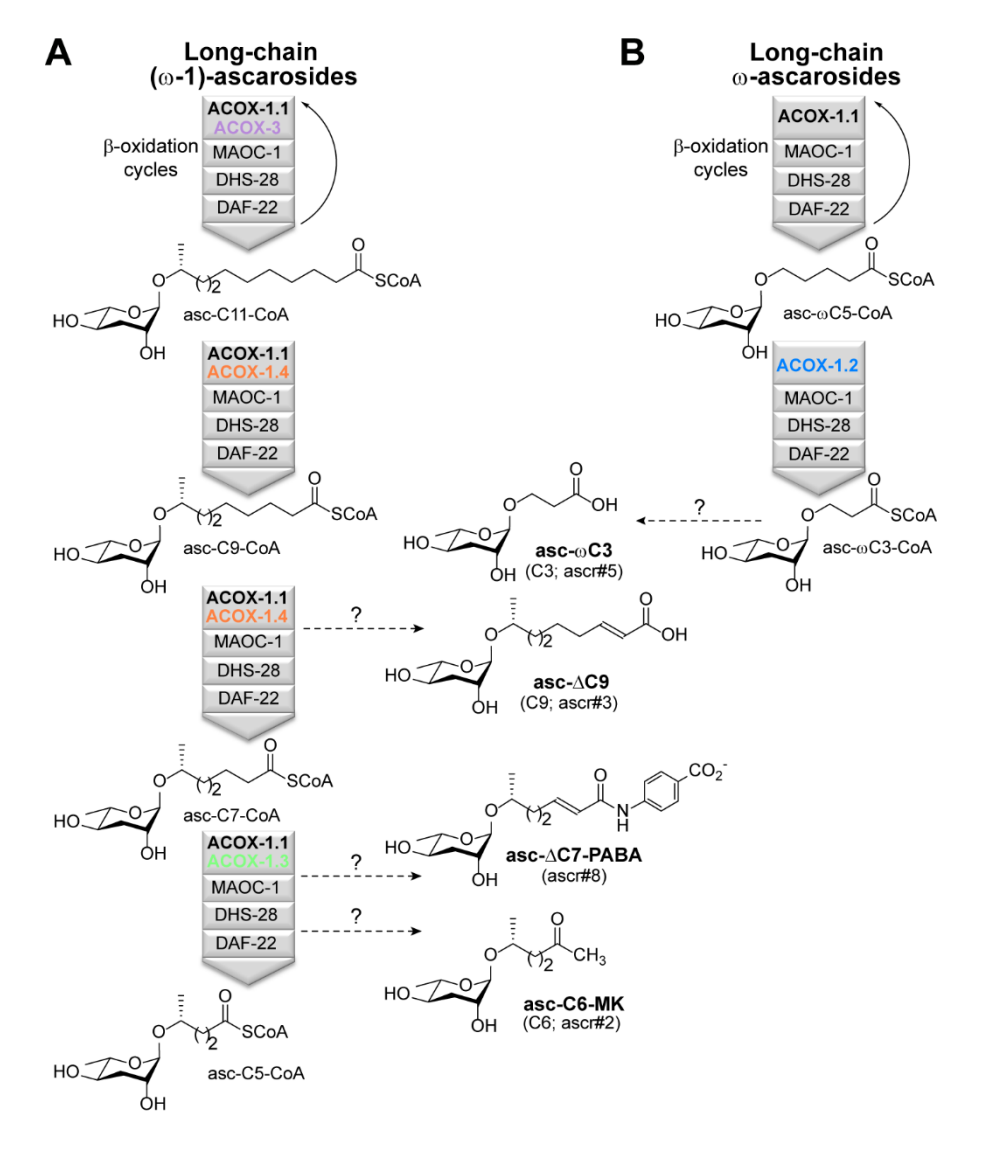


Figure 2. Model for the role of ACOX-1.1, ACOX-1.2, ACOX-1.3, ACOX-1.4, and ACOX-3 in the biosynthesis of (ω-1)-ascarosides (A) and ω-ascarosides (B) established in this paper. This model builds on the previously established roles of ACOX-1.1, -1.2, and -1.3 (previously known as ACOX-1, -2, and -3), ¹⁴ clarifies the role of ACOX-1.1, and uncovers the roles of ACOX-1.4 and ACOX-3 (which was previously known as ACOX-6). ¹⁵ The structures of four of the five dauer pheromone ascarosides are shown in between parts (A) and (B), and their likely biosynthetic pathways are indicated.

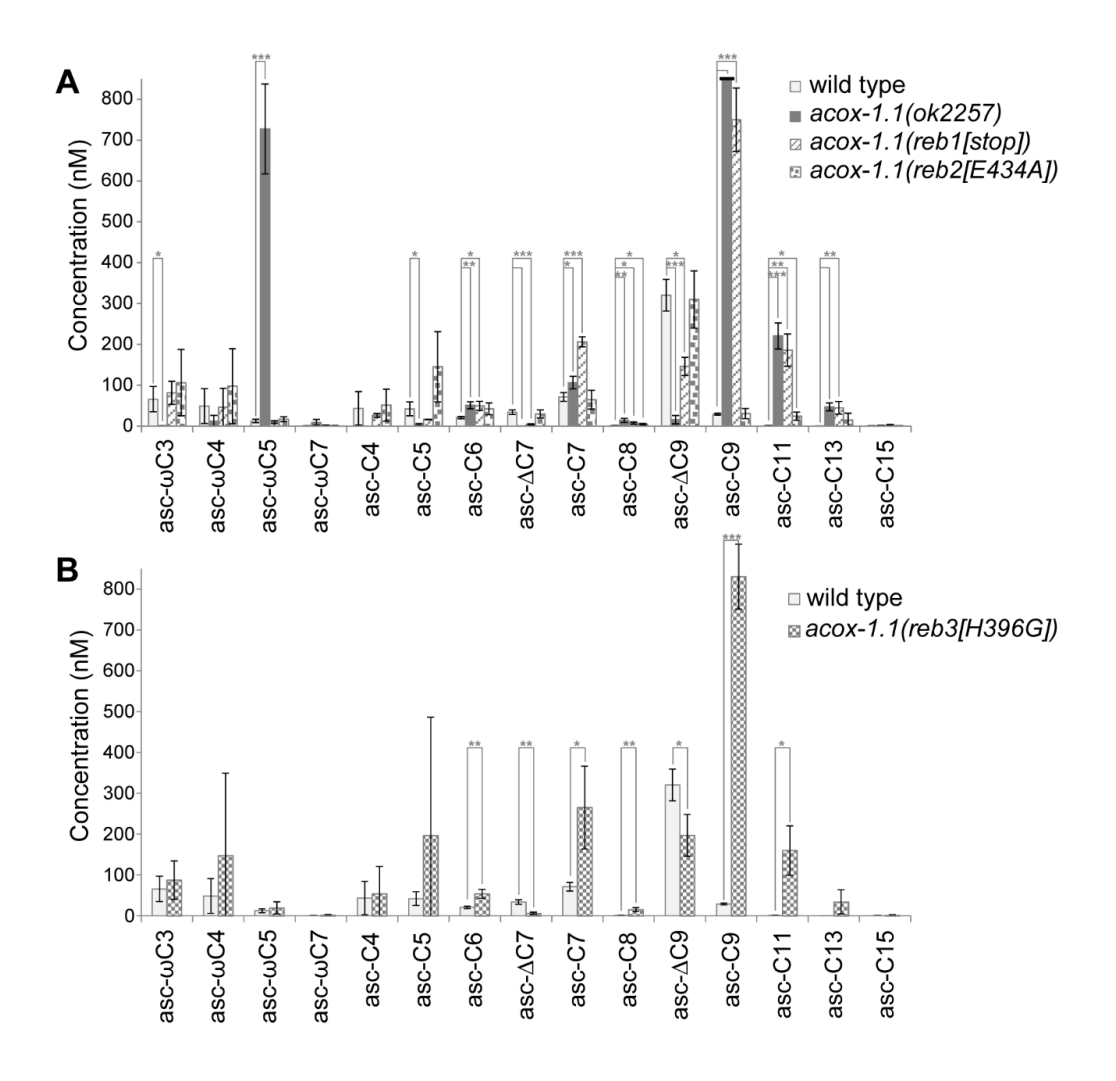


Figure 3. Ascaroside production in deletion, nonsense, and missense mutants of the acyl-CoA oxidase gene acox-1.1. (A) Ascaroside production in wild type, the acox-1.1(ok2257) deletion mutant, the acox-1.1(rab1, stop) nonsense mutant, and the acox-1.1(rab2, E434A) catalytic mutant. (B) Ascaroside production in wild type and the acox-1.1(rab3, H396G) ATP-binding mutant. Data in (A) and (B) represent the mean \pm SD of three independent experiments. Two-tailed, unpaired t-tests were used to determine statistical significance (* $P \le 0.05$, ** $P \le 0.01$, *** $P \le 0.001$).

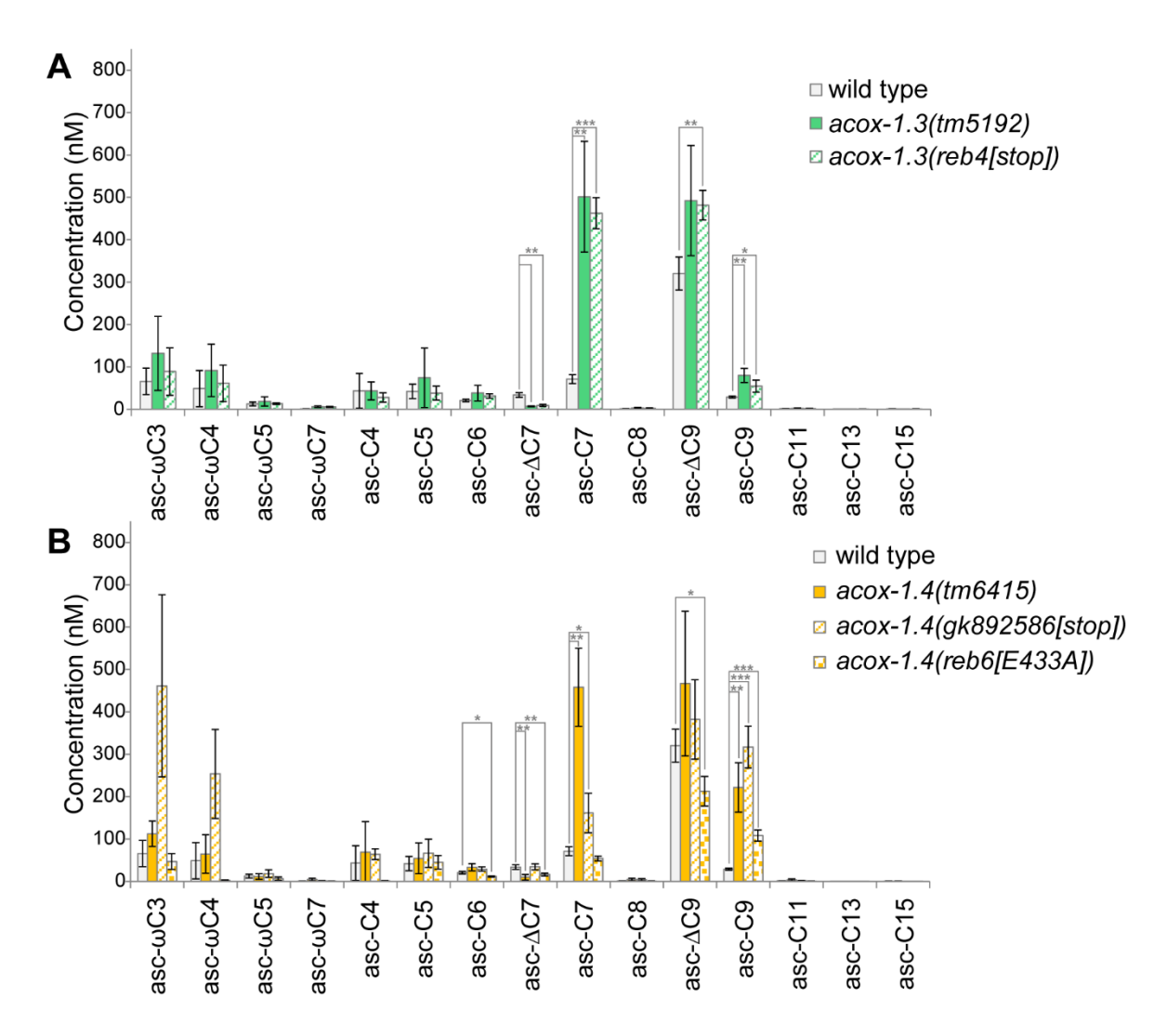


Figure 4. Ascaroside production in deletion, nonsense, and missense mutants of the acyl-CoA oxidase genes acox-1.3 and acox-1.4. (A) Ascaroside production in wild type, the acox-1.3(tm5192) deletion mutant, and the acox-1.3(rab4, stop) nonsense mutant. (B) Ascaroside production in wild type, the acox-1.4(tm6415) deletion mutant, the acox-1.4(gk892586, stop) nonsense mutant, and the acox-1.4(rab6, E433A) catalytic mutant. Data in (A) and (B) represent the mean \pm SD of three independent experiments. Two-tailed, unpaired t-tests were used to determine statistical significance (* $P \le 0.05$, ** $P \le 0.01$, *** $P \le 0.001$, *** $P \le 0.0001$).

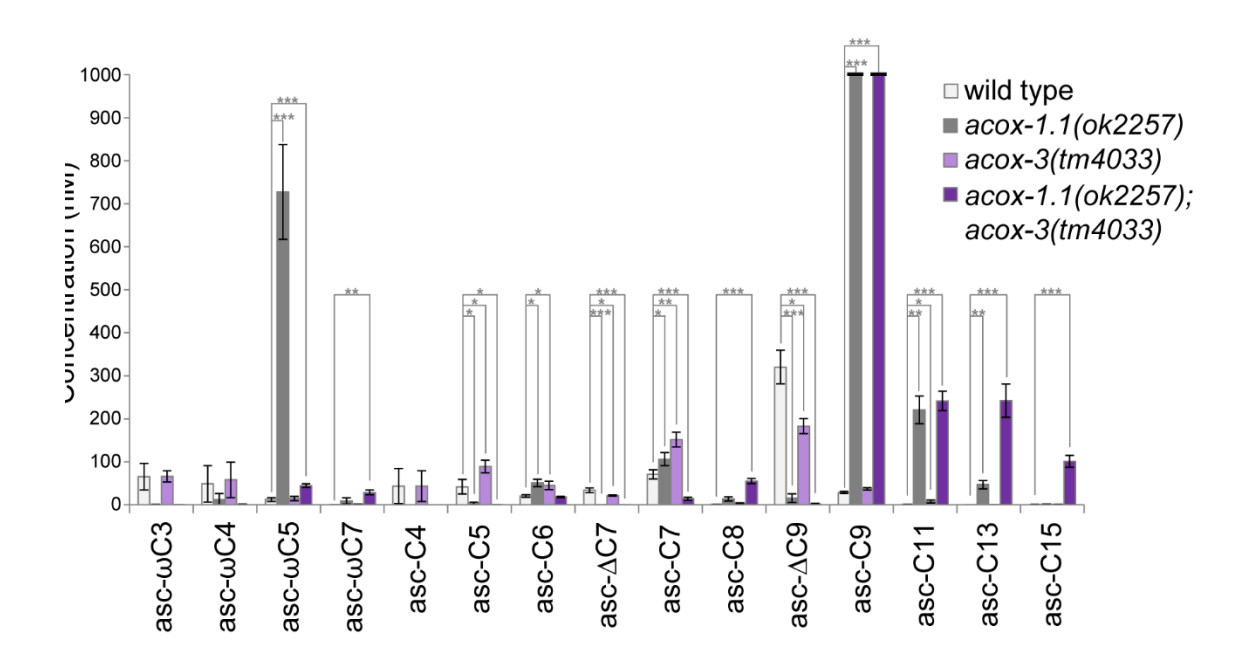


Figure 5. Ascaroside production in deletion mutants of the acyl-CoA oxidase genes acox-1.1 and acox-3. Ascaroside production in wild type, the acox-1.1(ok2257) deletion mutant, the acox-3(tm4033) deletion mutant, and the acox-1.1(ok2257); acox-3(tm4033) double deletion mutant. Data represent the mean \pm SD of three independent experiments. Two-tailed, unpaired t-tests were used to determine statistical significance (* $P \le 0.05$, ** $P \le 0.01$, *** $P \le 0.001$).

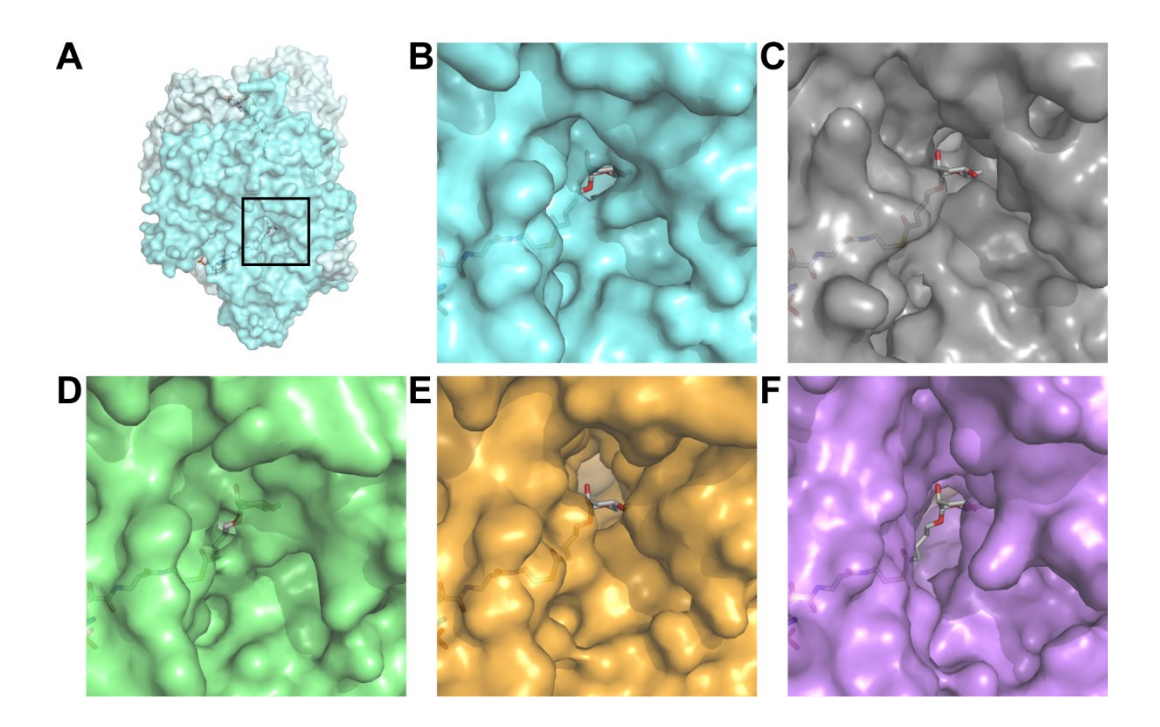


Figure 6. The X-ray crystal structures and modeled structures of acyl-CoA oxidases. (A) The crystal structure of the ACOX-1.2 homodimer with the bound ascaroside substrate, asc-ωC5-CoA (see Figure 2B for chemical structure). (B) A close-up of the boxed portion of the structure indicated in (A). (C) Close-up image of the crystal structure of the ACOX-1.1 homodimer, with the ascaroside substrate from the ACOX-1.2 structure placed in the active site to indicate the active site location. (D-F) Close-up images of the modeled structures of the ACOX-1.3 (D), ACOX-1.4 (E), and ACOX-3 (F) homodimers, with the ascaroside substrate from the ACOX-1.2 structure placed in the active sites to indicate the active site location.

Supplementary Information for

Acyl-CoA oxidases fine-tune the production of ascaroside pheromones with specific side chain lengths

Xinxing Zhang†, Yuting Wang†, David H. Perez, Rachel A. Jones Lipinski, and Rebecca A. Butcher*

Department of Chemistry, University of Florida, Gainesville, FL, United States

*E-mail: <u>butcher@chem.ufl.edu</u>

†X.Z. and Y.W. contributed equally to this work.

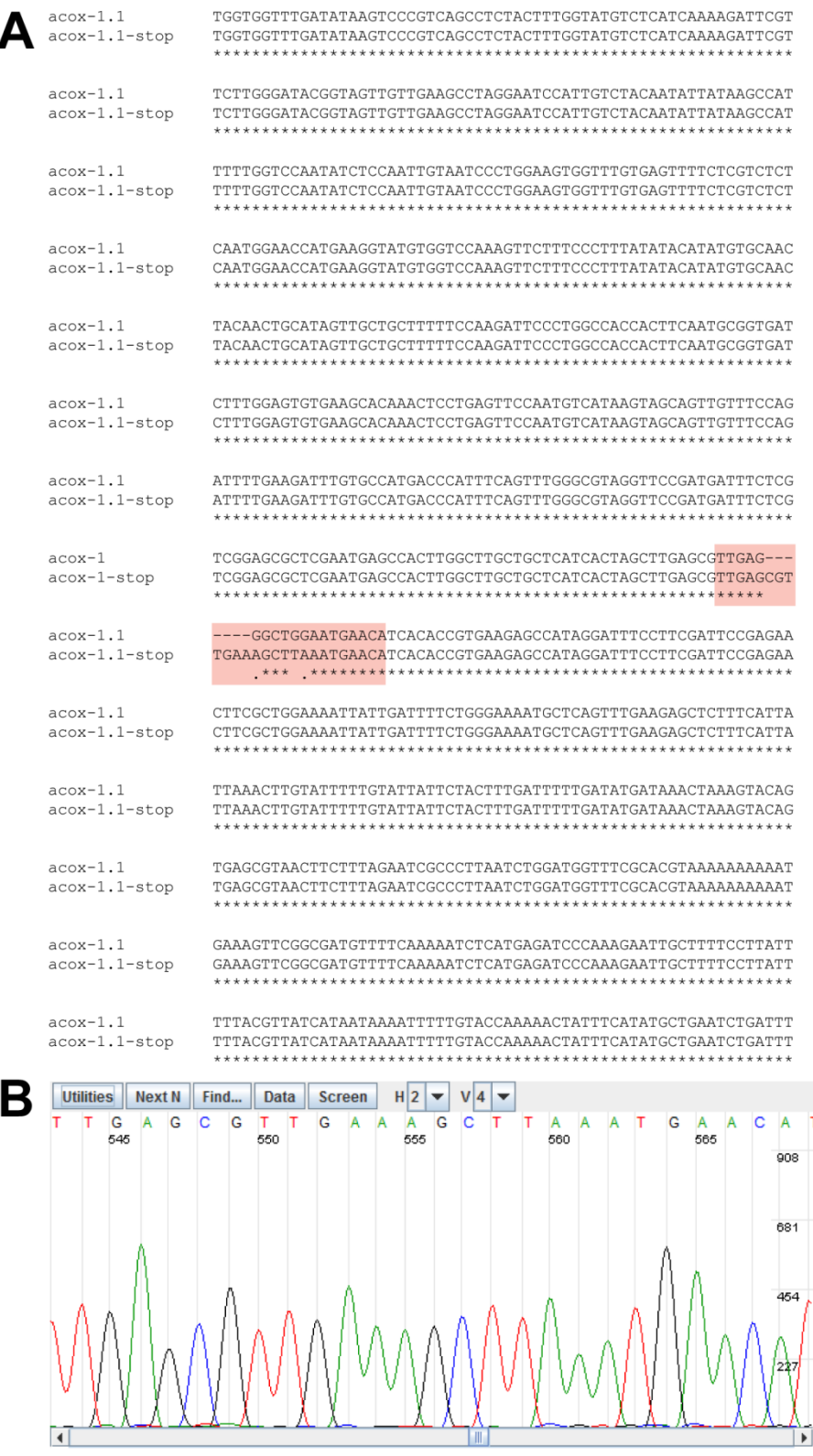


Figure S1. Sequencing data for acox-1.1(reb1[stop]). A. Alignment of sequence file with wild-type acox-1.1 gene sequence (reverse complement). Red box indicates location of trace shown in (B). Note that the strain also has a seven base insertion just 3' to the stop codon (TAA). B. Portion of sequencing trace for acox-1.1(reb1[stop]).

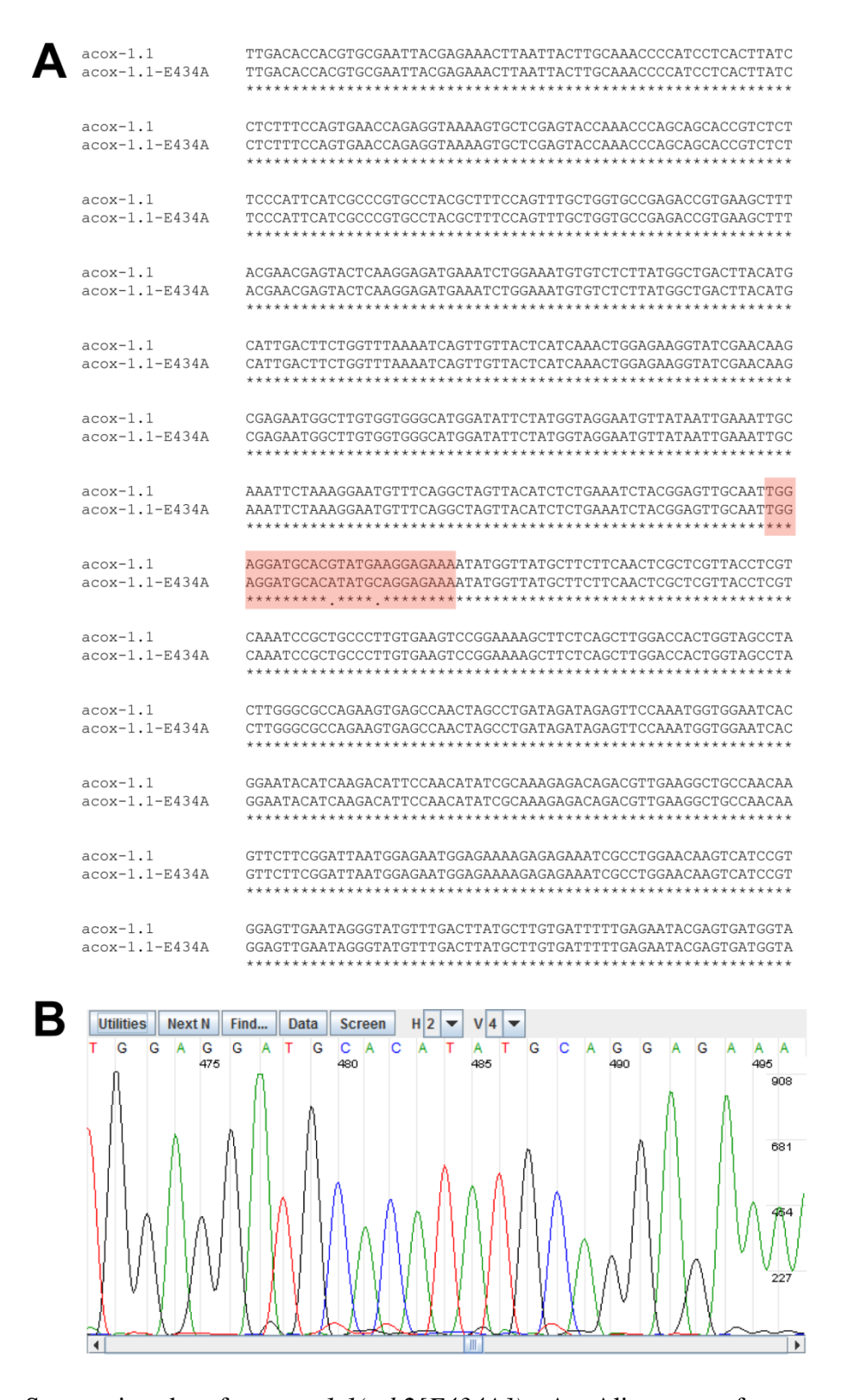


Figure S2. Sequencing data for acox-1.1(reb2[E434A]). A. Alignment of sequence file with wild-type acox-1.1 gene sequence. Red box indicates location of trace shown in (B). B. Portion of sequencing trace for acox-1.1(reb2[E434A]).

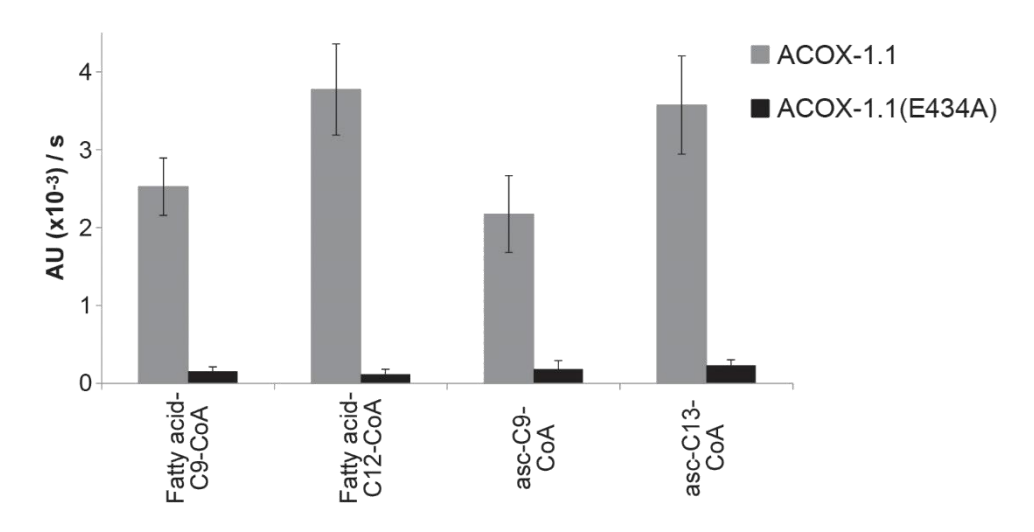


Figure S3. *In vitro* activity of wild-type ACOX-1.1 and an ACOX-1.1(E434A) catalytic mutant towards different substrates. Data represent the mean \pm SD of two independent experiments.

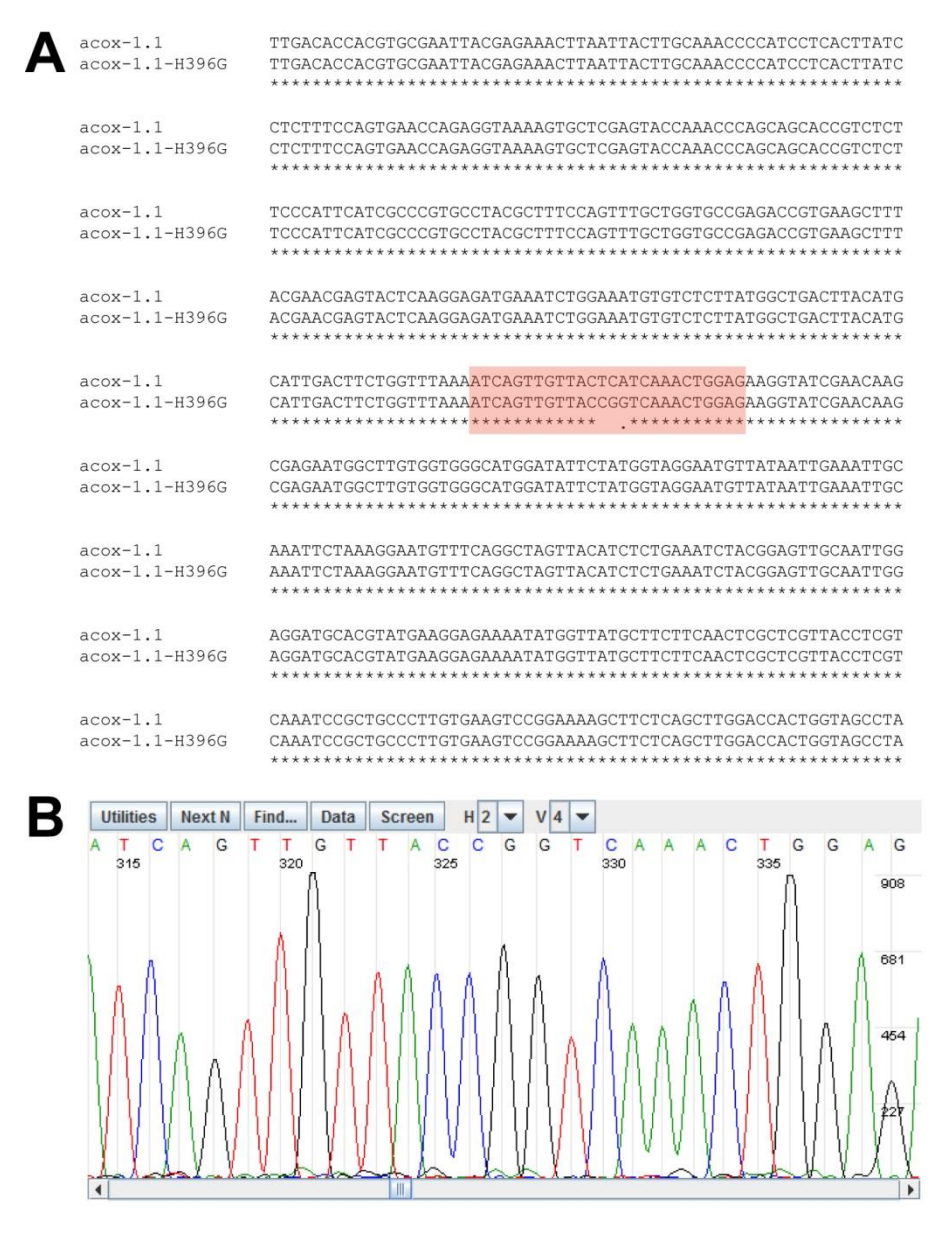


Figure S4. Sequencing data for acox-1.1(reb3[H396G]). A. Alignment of sequence file with wild-type acox-1.1 gene sequence. Red box indicates location of trace shown in (B). B. Portion of sequencing trace for acox-1.1(reb3[H396G]).

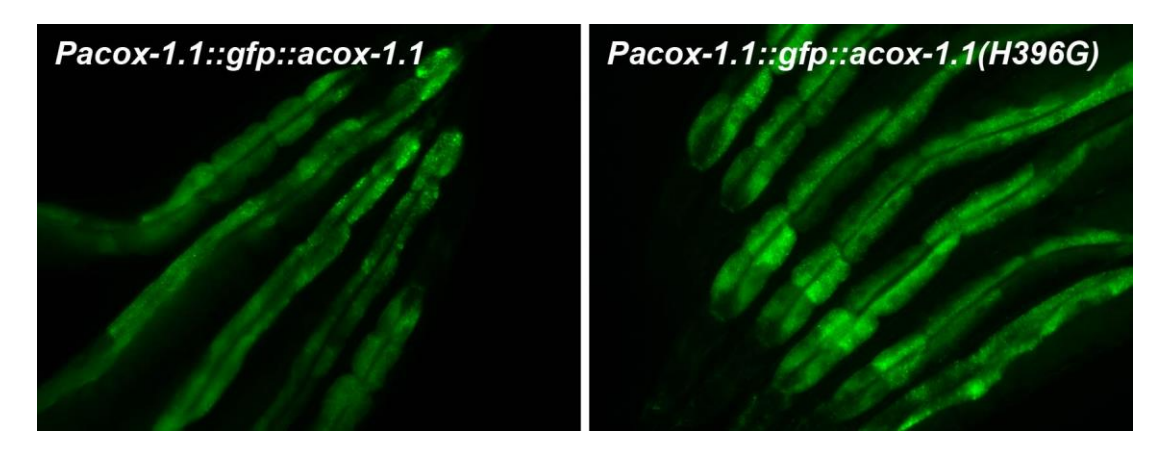


Figure S5. Fluorescence microscopy of the *Pacox-1.1::gfp::acox-1.1* and *Pacox-1.1::gfp::acox-1.1(H396G)* translational reporter strains.

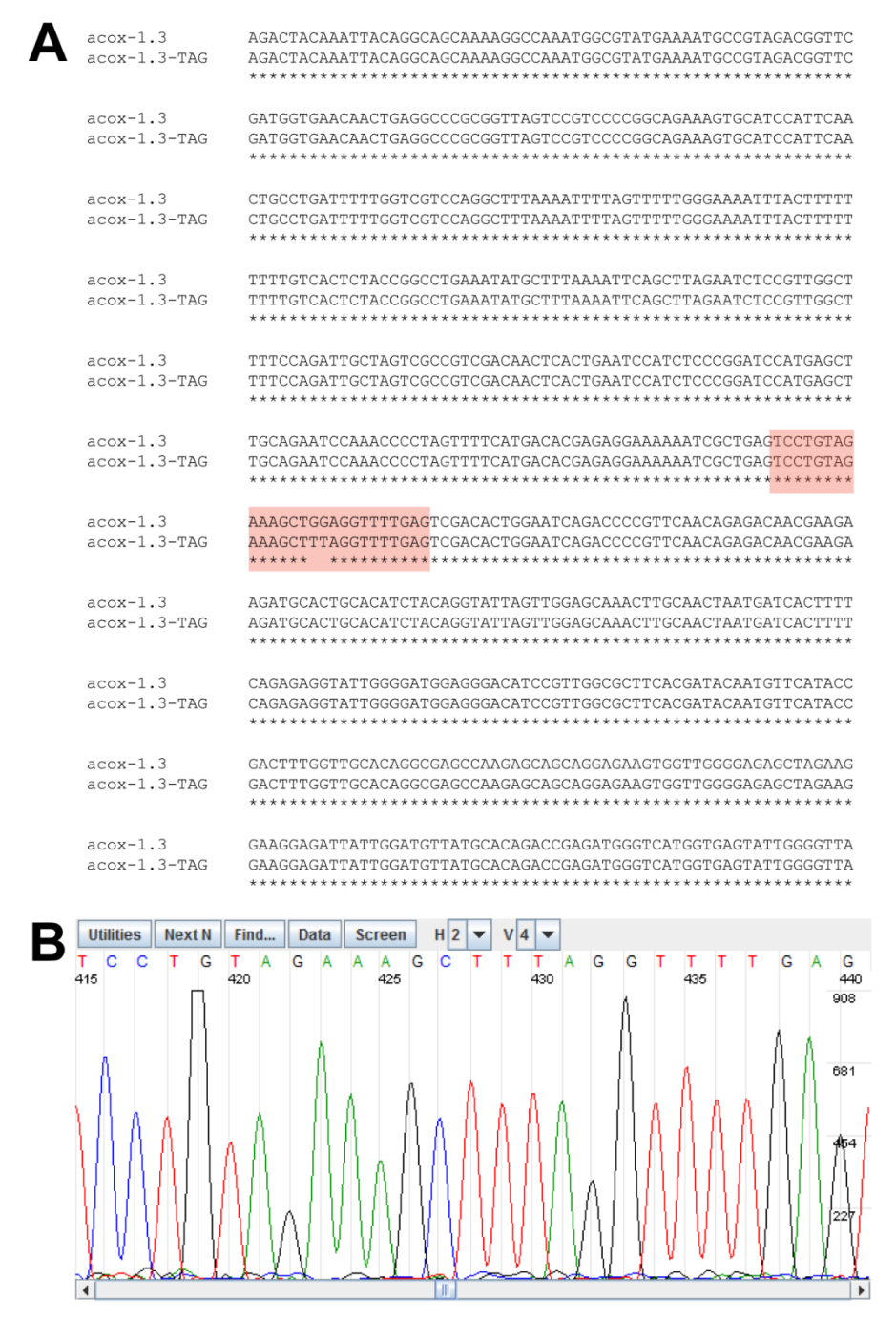


Figure S6. Sequencing data for *acox-1.3(reb4[stop])*. A. Alignment of sequence file with wild-type *acox-1.3* gene sequence. Red box indicates location of trace shown in (B). B. Portion of sequencing trace for *acox-1.3(reb4[stop])*.

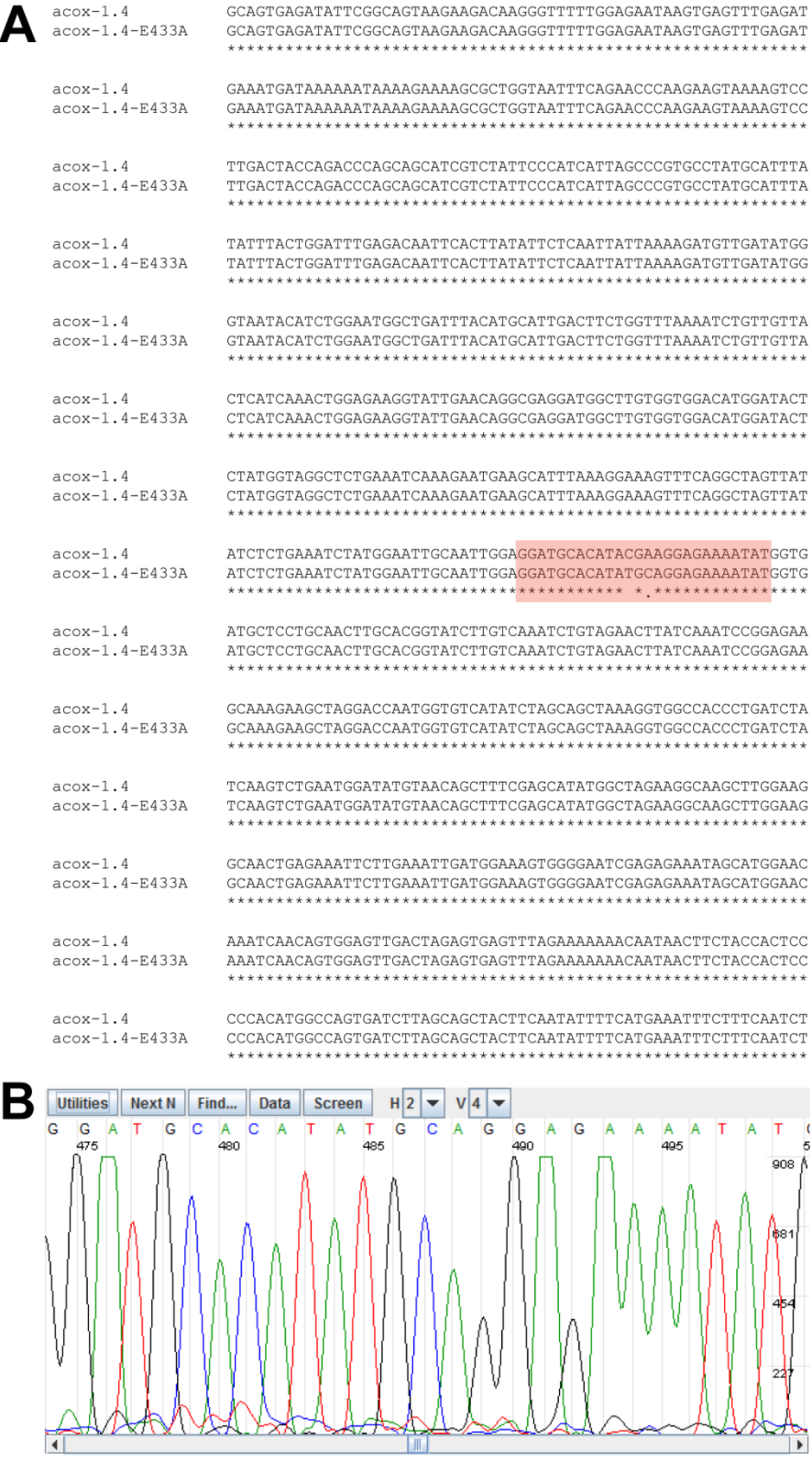


Figure S7. Sequencing data for acox-1.4(reb6[E433A]). A. Alignment of sequence file with wild-type acox-1.4 gene sequence. Red box indicates location of trace shown in (B). B. Portion of sequencing trace for acox-1.4(reb6[E433A]).

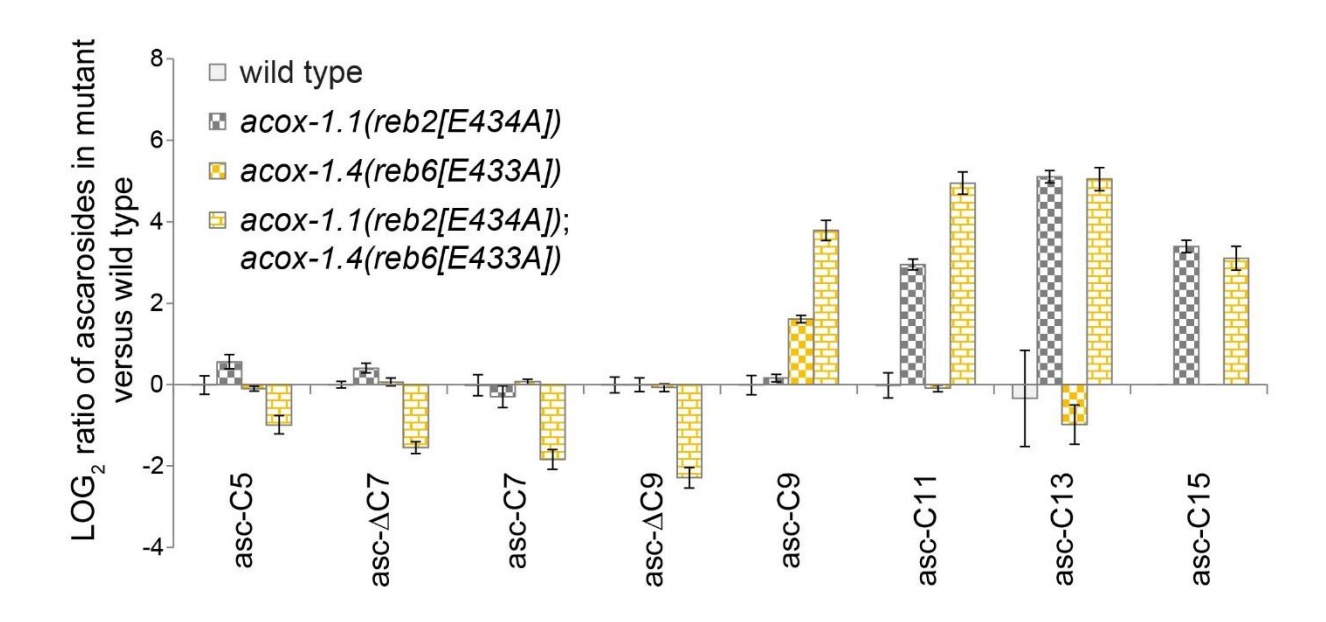


Figure S8. Ascaroside production in wild type, the acox-1.1(reb2[E434A]) catalytic mutant, the acox-1.4(reb6[E433A]) catalytic mutant, and the acox-1.1(reb2[E434A]); acox-1.4(reb6[E433A]) double mutant. Log ratio of ascaroside production in wild type and mutants, relative to wild type. For ascarosides that could not be detected, their peak area was set at the detection limit of the LC-MS. Data represent the mean \pm SD of three independent experiments.

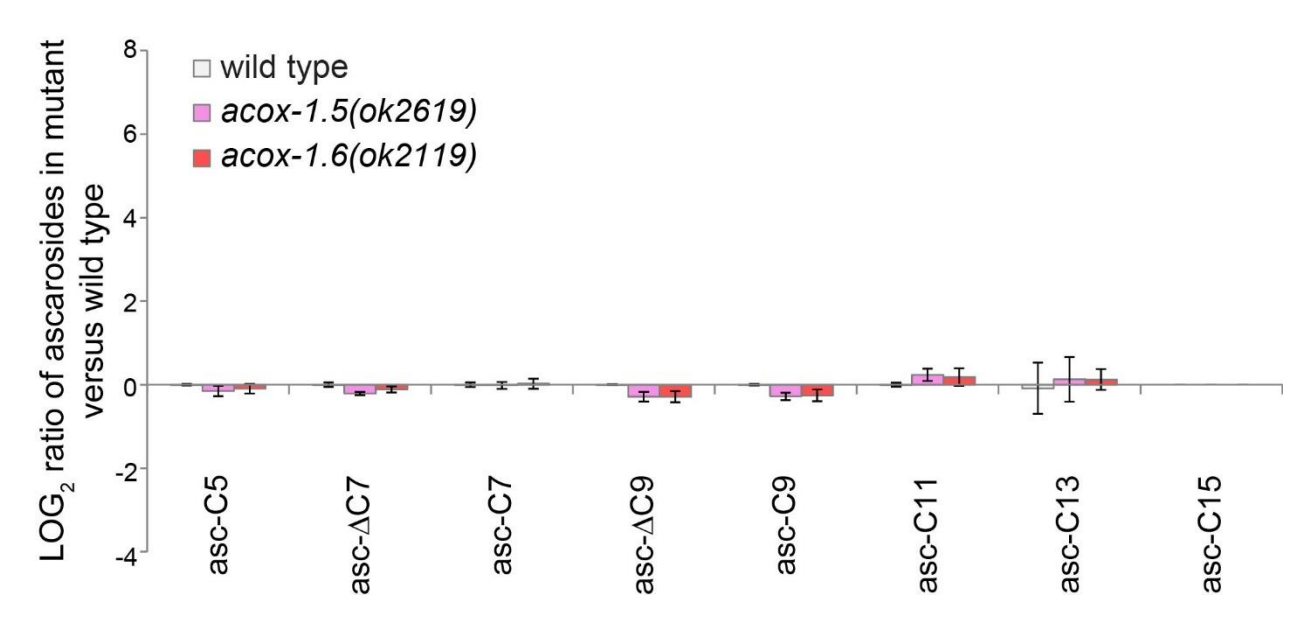


Figure S9. Ascaroside production in wild type, the acox-1.5(ok2619) deletion mutant, and the acox-1.6(ok2119) deletion mutant. Log ratio of ascaroside production in wild type and mutants, relative to wild type. For ascarosides that could not be detected, their peak area was set at the detection limit of the LC-MS. Data represent the mean \pm SD of three independent experiments.

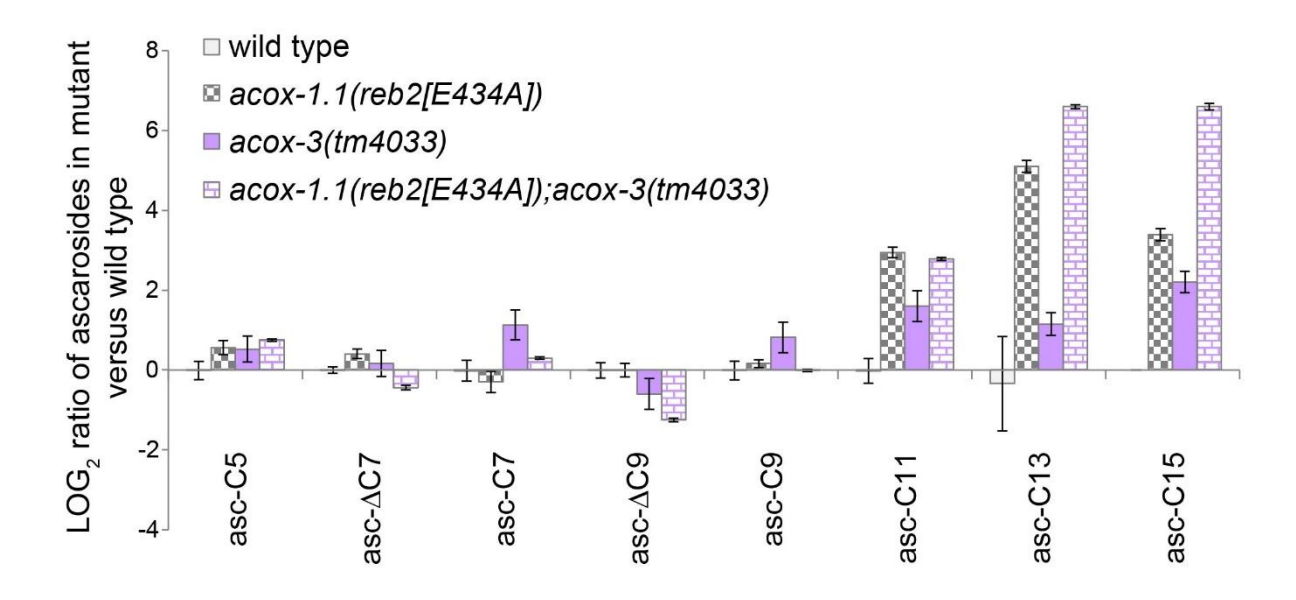


Figure S10. Ascaroside production in wild type, the acox-1.1(reb2[E434A]) catalytic mutant, the acox-3(tm4033) deletion mutant, and the acox-1.1(reb2[E434A]); acox-3(tm4033) double mutant. Log ratio of ascaroside production in wild type and mutants, relative to wild type. For ascarosides that could not be detected, their peak area was set at the detection limit of the LC-MS. Data represent the mean \pm SD of three independent experiments.

Table S1. ACOX new and previous nomenclature.

New Nomenclature	Previous Nomenclature
ACOX-1.1	ACOX-1
ACOX-1.2	ACOX-2
ACOX-1.3	ACOX-3
ACOX-1.4	ACOX-4
ACOX-1.5	ACOX-5
ACOX-1.6	unnamed (F59F4.1)
ACOX-3	ACOX-6